This a pre-print version.
The final document is available at http://www.springerlink.com

# Which reorientation framework for the atlas-based comparison of cardiac image sequences?

Nicolas Duchateau[1], Mathieu De Craene[2], Xavier Pennec[3], Beatriz Merino[1], Marta Sitges[1], and Bart Bijnens[4]

[1] Hospital Clínic - IDIBAPS - Universitat de Barcelona, Spain
[2] Philips Research, Medisys, Suresnes, France
[3] Asclepios Team Project, INRIA Sophia Antipolis Méditerranée, France
[4] Universitat Pompeu Fabra - ICREA, Barcelona, Spain

**Abstract.** The present paper builds upon recent advances in the spatiotemporal alignment of cardiac sequences to construct a statistical atlas of normal motion. Comparing cardiac sequences requires considering both the temporal component (changes along the sequences) and the inter-subject one. The objective here is to understand the changes in the comparison of myocardial velocities depending on (1) the chosen reorientation action (*finite strain* [local rotation only], *local rotation and isotropic scaling*, or full Jacobian matrix using the *push-forward*) and (2) the chosen system of coordinates (*Lagrangian*, *Eulerian*, or if a compromise between both [e.g. *hybrid-Eulerian*] is possible). Myocardial velocities are estimated locally using speckle tracking on echocardiographic (US) sequences, then aligned to a reference timescale, and finally reoriented to the anatomical reference according to the chosen reorientation framework. The methodology was applied to 2D US sequences in a 4-chamber view from 71 healthy volunteers. Experiments highlight the limitations of the *hybrid-Eulerian* scheme, showing that the intra-subject transformation should be taken into account, and discuss the options to perform the inter-subject one.

## 1 Introduction

Despite the large advances realized during the last decade on the understanding of cardiac function, motion and deformation, and the etiologies of cardiac dyssynchrony, the clinical applicability of myocardial motion and deformation comparison techniques remains limited. The abundance of publications performing single-parameter measurements of e.g. dyssynchrony (time-to-peak or time-to-onset indexes, in a majority) or other clinical and image-based parameters, including promising and extensively advertised (but deceiving) large-scale multicenter studies, largely contributed to this [11].

On a technical point-of-view, methods derived from recent advances in computational anatomy [21] and statistical atlases [28] [32] are particularly of interest for performing the above-mentioned comparison: they define (1) a common

This a pre-print version.
The final document is available at http://www.springerlink.com



anatomical reference where statistics can be performed and (2) a framework to transport the studied data (shape or the information defined at each point of this shape) to this anatomical reference.

The characterization of myocardial motion and deformation patterns requires a quantitative comparison of cardiac image sequences, i.e. high dimensional and temporally evolving information. In neuroimaging applications, which represent a majority of the current applications of computational anatomy, temporal dimension of the data stands for longitudinal studies. Challenges in this context differ from cardiac studies, and the focus is on growth processes, with few temporal samples for each subject. For this application, aligning the information to baseline time $t = 0$ seems the most relevant choice. In contrast, studying cardiac function supposes looking at cyclic information with much more temporal samples for each subject (from 20 to over 100 images per cycle in 2D ultrasound [US] sequences). Note that longitudinal studies also exist in cardiac applications, when looking at the evolution of the cardiac function of one subject at different stages, e.g. before and after the therapy.

The statistical comparison of cardiac sequences can be performed in the reference anatomy, either at each temporal instant (*Eulerian* framework), or at the time-point initiating the sequences (*Lagrangian* framework). Both strategies have been adopted in the literature about statistical atlases built for longitudinal or temporal data (*Eulerian*: [5] [10] [13] [16]) or (*Lagrangian*: [15] [26] [27] [18] [19] [23]), and require transporting the information along the sequences to the chosen system of coordinates. This can be directly achieved by means of resampling, if the transported information is scalar, or by resampling and local reorientation in case the transported information is vectorial. The *Eulerian* and *Lagrangian* frameworks, numerical approximations apart [4], should lead to similar results, and the observed differences should only reflect that the comparison between subjects is done in a different system of coordinates.

In the present work, we build upon recent methods targeting the spatiotemporal alignment of cardiac sequences [24] [25], and raise the two following questions concerning the reorientation process:

• In neuroimaging applications, intra-sequence transformations have smaller magnitude than inter-sequence ones. Is this the case for cardiac studies, and is the inclusion of intra-sequence transformations really necessary?

• What is the influence of the reorientation action on the comparison between subjects, and which one should be preferred?

We discuss these aspects through the construction of a statistical atlas of myocardial velocities built from 2D US sequences (4-chamber view) from 71 healthy volunteers, using a framework adapted from [9].

## 2 Methods

### 2.1 Intra-sequence registration

The myocardial wall is tracked along a given 2D US sequence using a speckle tracking [20] algorithm from commercial software (Echopac software v.110.1.2,

This a pre-print version.
The final document is available at http://www.springerlink.com



GE Healthcare, Milwaukee, WI, USA), which propagates a segmentation of the myocardium along the whole sequence (Fig. 1). In our protocol, the myocardial wall is manually segmented at end-systole using a control-point-based delineation of the endocardium (starting from the mitral valve level and first covering the septum) and the choice of a wall-thickness, as required by the software interface.

The output of the speckle tracking software is the discrete position of the centerline of the myocardium along the whole sequence, in cartesian coordinates, and is used as input for the algorithms we developed to compute myocardial velocities. In our implementation, drift compensation is used to guarantee cyclic motion, and no additional spatiotemporal smoothness is added than the one inherent to the speckle tracking algorithm. Radial and longitudinal directions are computed locally from the discrete centerline of the myocardium (Fig. 1).

Myocardial displacements are computed at each point of the centerline, as the difference of its position at times 0 and $t$. *Eulerian* myocardial velocities are obtained from the temporal derivative of the displacements. This is possible under the assumption that the displacements between consecutive frames are small, as justified in [9]. In the following, we denote $\mathbf{v}^k(\mathbf{x}, t)$ the velocities for subject $k$ at the observed spatiotemporal location $(\mathbf{x}, t)$.

**Choice of speckle tracking against image-based registration.** The concept of the speckle tracking algorithm is similar to the tracking achieved through image registration along cardiac sequences, with the specificity of computing image similarities locally (tracking local speckle pattern). Although few details are given by the manufacturer regarding its implementation, we believe the algorithm to follow the principles given in [2] [1] [17]. It has the advantage of being fast (around $2-3$ $s$ per cardiac sequence), and widely used in the clinical community, which is the reason why we chose to use it. Note that further validation is actively required by the clinical international associations [22].

However, the choice of using this tracking technique conditions the reorientation process described in this paper. Registration-based methods provide a dense transformation, the local Jacobian of which can be used in the reorientation process (*push-forward action* [30], which includes both radial and longitudinal components of the intra- and inter-subject mappings). In contrast, the current version of the speckle tracking software only provides the position of the centerline of the myocardium, and simpler reorientation actions should be considered (*finite strain* [local rotation only], and *local rotation and isotropic scaling*). The reorientation process is detailed further in this paper (Sec. 2.3).

### 2.2 Temporal alignment

Myocardial velocities are temporally aligned to a common timescale using piecewise-linear warping of the timescale based on the timing of the following physiological events [9]:

- The *onset of the QRS complex*, directly identified on the ECG curve.

This a pre-print version.
The final document is available at http://www.springerlink.com



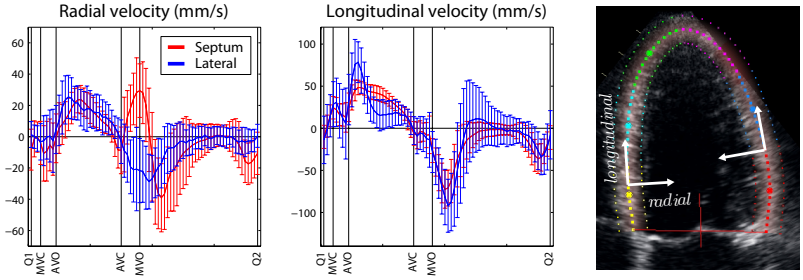


**Fig. 1:** Left: Radial and longitudinal myocardial velocities at mid inferoseptal (red) and anterolateral (blue) levels. Average ± standard deviation over the set of healthy volunteers. *Eulerian* scheme, first choice of reorientation action (*local rotation only*), see Sec. 2.3 and 2.3 for details. Right: Myocardial segmentation (end-systole) used for the speckle tracking algorithm. Note that only the position of the myocardial centerline is available with the current version of the software (Sec. 2.1)

• The *opening and closure of the aortic and mitral valves* (AVO, AVC, MVO and MVC) determined using continuous wave Doppler imaging on the corresponding valve.

### 2.3 Spatial alignment

**Resampling.** For all the choices of reorientation action and system of coordinates (see below for details), prior resampling is required.

Cubic spline interpolation is used to have an approximation of the velocities on a continuous timescale, as these are initially defined at the discrete temporal samples of each sequence. The choice of the temporal interpolation technique clearly influences the accuracy of the atlas computations [8], and more elaborated methods could be used for this (in particular, compliant with the diffeomorphic framework, namely the definition of displacements as the flow of time-dependent velocity fields [e.g. diffeomorphic-compliant spline interpolation [29] [31], or temporal diffeomorphic free-form-deformation [7], [6]]), but we preferred a simpler (and faster) scheme for the work presented in this paper.

Cubic spline interpolation is also used to have a continuous approximation of the velocities along the whole centerline of the myocardium, as these are initially defined at the discrete locations provided by the speckle tracking algorithm, the number of which being different for each sequence.

**Reorientation action.** Spatial normalization consists in locally reorienting the computed velocity fields $\mathbf{v}^k(\mathbf{x}, t)$, initially defined with respect to the anatomy of subject $k$, to a reference anatomy, using:

$$P(\mathbf{v}) = \mathbf{A}(\varphi^{k \to ref}(\mathbf{x}, t)) \cdot \mathbf{v}, \tag{1}$$

This a pre-print version.
The final document is available at http://www.springerlink.com



where $\mathbf{v} = \mathbf{v}^k(\mathbf{x}, t)$, $\varphi^{k \to ref}(\mathbf{x}, t)$ is the estimated mapping to the reference, and $\mathbf{A}(\varphi^{k \to ref}(\mathbf{x}, t))$ is the chosen reorientation action (2D matrix). The reference is selected using the group-wise normalized mutual information metric [14].

As introduced at the end of Sec. 2.1, several choices of reorientation action are possible:

• *Finite strain*: the simplest option considers reorientation as local rotation only, and $\mathbf{A}(\varphi^{k \to ref}(\mathbf{x}, t))$ is therefore a rotation matrix. In general, the rotation part of the local deformation is obtained by taking the polar decomposition of the Jacobian matrix, hence the name finite strain reorientation coined in diffusion tensor (DTI) registration. In our case, we do not have access to the Jacobian matrix but we can easily estimate the rotation directly from the motion of the neighboring centerline points.

• The previous case does not take into account that the heart size and shape may differ between subjects. A second reorientation option would therefore consist in *local rotation and isotropic scaling*, adding to the above-mentioned rotation matrix a local scaling factor. In general, this factor can be chosen to be the mean scaling of the Jacobian matrix along each direction. Here, this factor is estimated from the spacing between the centerline points neighboring the location $(\mathbf{x}, t)$ in the anatomy of subject $k$ and the reference one. It would correspond to the longitudinal-longitudinal component of $\mathbf{D}\varphi^{k \to ref}(\mathbf{x}, t)$ ($\mathbf{D}$ being the Jacobian operator), if the transform $\varphi^{k \to ref}(\mathbf{x}, t)$ was available over at least a neighborhood of the myocardial centerline.

• *Push-forward*: the last option estimates the whole Jacobian of $\varphi^{k \to ref}(\mathbf{x}, t)$, therefore setting $\mathbf{A}(\varphi^{k \to ref}(\mathbf{x}, t)) = \mathbf{D}\varphi^{k \to ref}(\mathbf{x}, t)$. This is generally achieved in the literature by means of registration techniques (e.g. the pipeline our present work is based upon used image-based registration [9]). This does not apply in our case, as discussed at the end of Sec. 2.1, as the myocardial centerline is the only output from the speckle tracking algorithm. A partial alternative could consist in estimating a smooth transformation from the set of landmarks defining the centerline (for which the correspondence is known), using the landmark-case option of the algorithm of [12] (according to the implementation available online at `http://www.mi.parisdescartes.fr/~glaunes/matchine.zip`) . Note that the accuracy of this process is highly conditioned by the smoothness imposed to the estimated transformations.

**Which system of coordinates?** As mentioned in the introduction, we can distinguish between comparing the data in the reference anatomy at time $t = 0$ or $t \neq 0$, according to the following two schemes:

• *Lagrangian* framework (mapping to the reference at time $t = 0$):

$$\varphi^{k \to ref}(\mathbf{x}, t) = \varphi^{k \to ref}(., 0) \circ \varphi^k_{t \to 0}(\mathbf{x}), \tag{2}$$

where $\varphi^k_{t \to 0}$ is the transformation between times 0 and $t$ within the sequence of subject $k$.

• *Eulerian* framework (mapping to the reference at time $t \neq 0$):

$$\varphi^{k \to ref}(\mathbf{x}, t) = \varphi^{ref}_{0 \to t} \circ \varphi^{k \to ref}(., 0) \circ \varphi^k_{t \to 0}(\mathbf{x}). \tag{3}$$

This a pre-print version.
The final document is available at http://www.springerlink.com



When using the full Jacobian with the *push-forward*, we would therefore have:

$$\begin{aligned} \mathbf{D}(\varphi^{k\to ref}(\mathbf{x},t)) &= \mathbf{D}_2 \cdot \mathbf{D}_3 \qquad \text{(Lagrangian scheme)},\\ \text{or } \mathbf{D}(\varphi^{k\to ref}(\mathbf{x},t)) &= \mathbf{D}_1 \cdot \mathbf{D}_2 \cdot \mathbf{D}_3 \qquad \text{(Eulerian scheme)}, \end{aligned}$$

with

$$\begin{aligned} \mathbf{D}_1 &= \mathbf{D}\big(\varphi^{ref}_{0\to t}\big)\big(\varphi^{k\to ref}(.,0)\circ\varphi^{k}_{t\to 0}(\mathbf{x})\big)\\ \mathbf{D}_2 &= \mathbf{D}\big(\varphi^{k\to ref}(.,0)\big)\big(\varphi^{k}_{t\to 0}(\mathbf{x})\big)\\ \mathbf{D}_3 &= \mathbf{D}\big(\varphi^{k}_{t\to 0}\big)\big(\mathbf{x}\big). \end{aligned} \tag{4}$$

Now, taking another reorientation action $\mathbf{A}(\varphi^{k\to ref}(\mathbf{x},t))$, we could decide to use $\mathbf{A}(\mathbf{D}_1\cdot\mathbf{D}_2\cdot\mathbf{D}_3)$ or $\mathbf{A}(\mathbf{D}_1)\cdot\mathbf{A}(\mathbf{D}_2)\cdot\mathbf{A}(\mathbf{D}_3)$, or possibly neglect the rotation along the time sequence, which means approximating $\mathbf{A}(\mathbf{D}_1)$ and $\mathbf{A}(\mathbf{D}_3)$ by the identity matrix, i.e. taking $\mathbf{A}(\mathbf{D}_1\cdot\mathbf{D}_2\cdot\mathbf{D}_3)\approx\mathbf{A}(\mathbf{D}_2)$. We denote this scheme the *hybrid-Eulerian* framework. Note that a *hybrid-Lagrangian* framework is also possible.

### 2.4 Statistical comparison

Due to the assumption made about small displacements (Sec. 2.1), classical statistics can be computed directly on the aligned velocity fields. At a given location $(\mathbf{x},t)$, the average $\bar{\mathbf{v}}$ and covariance matrix $\Sigma_{\mathbf{v}}$ of the velocities from a population of $K$ sequences are defined as:

$$\bar{\mathbf{v}} = \frac{1}{K}\sum_{k=1}^{K}\mathbf{v}^k \quad \text{and} \quad \Sigma_{\mathbf{v}} = \frac{1}{K-1}\mathbf{V}^t\cdot\mathbf{V}, \tag{5}$$

where $\mathbf{V}^t = [(\mathbf{v}^1-\bar{\mathbf{v}})|\ldots|(\mathbf{v}^K-\bar{\mathbf{v}})]$.

## 3 Experiments and results

### 3.1 Echocardiographic data

Two-dimensional echocardiographic (2D US) image sequences from 71 healthy volunteers were acquired in an apical 4-chamber view using a GE Vivid 7 echographic system (GE Healthcare, Milwaukee, WI, USA). Enrollment criteria were that the subjects had no history of cardiac disease and a normal echocardiographic exam. All of them showed a QRS duration $< 120$ ms, and their baseline characteristics matched the values found in the literature for a population of patients with normal cardiac function. Images were acquired during breath-hold to minimize the influence of respiratory motion. Resolution was optimized during the acquisition, and corresponded to a frame rate of $71\pm15$ $fps$ (heart rate being of $66\pm12$) and a pixel size of $0.25\times0.25$ $mm^2$.

The research complied with the Declaration of Helsinki and the study protocol was accepted by our local ethics committee. Written informed consent was obtained from all subjects.

This a pre-print version.
The final document is available at http://www.springerlink.com



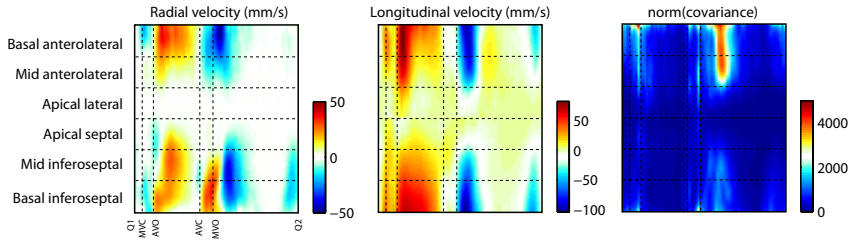


**Fig. 2:** Spatiotemporal maps used for the comparison of the reorientation frameworks. *Eulerian* scheme, first choice of reorientation action (*local rotation only*).

### 3.2 Which reorientation action and which system of coordinates?

In the following, we compare the three reorientation frameworks described in Sec. 2.3. Differences between the results obtained for each framework are represented by means of color-coded maps, in which the horizontal axis is time (one cardiac cycle, vertical dashed lines indicating the timing of the physiological events listed in Sec. 2.2, in the following order: onset of QRS, MVC, AVO, AVC, MVO, onset of QRS), and the vertical axis is the position along the myocardium (horizontal dashed lines indicating the separation between the myocardial segments). A similar display was used in [9] to represent myocardial motion abnormalities at each location in time and space. In the present paper, three different maps are represented: average radial and longitudinal velocities, and the norm of the local covariance matrix.

**Local rotation only.** We first computed the above-mentioned maps for the first option of reorientation action (*local rotation only*). Fig. 2 represents the maps for the *Eulerian* scheme, which will be used as reference for the comparison of the different reorientation frameworks. We can observe that the septal and lateral walls have similar motion (horizontal symmetry of the maps), reflecting the synchronicity in the cardiac contraction for the healthy volunteers. Lower velocities are observed near the apical level.

Very high variability is observed at the extremities of both septal and lateral walls (bottom and top rows of the map representing the norm of the covariance), reflecting the difficulty of tracking the basal myocardium, also affected by the presence of the mitral valve. A similar amount of variability is observed for the basal and mid anterolateral segments at early-diastole, reflecting the problem of properly imaging the lateral wall through the inaccuracies of the speckle tracking algorithm at this level (closeness of the lateral wall with the border of the field-of-view of 2D US images).

Apart from these regions with abnormally high variability, the highest variability is observed at early-systole, early-diastole and end-diastole, as assessed by the norm of the covariance. These correspond to zones where the myocardial acceleration is higher.

This a pre-print version.
The final document is available at http://www.springerlink.com



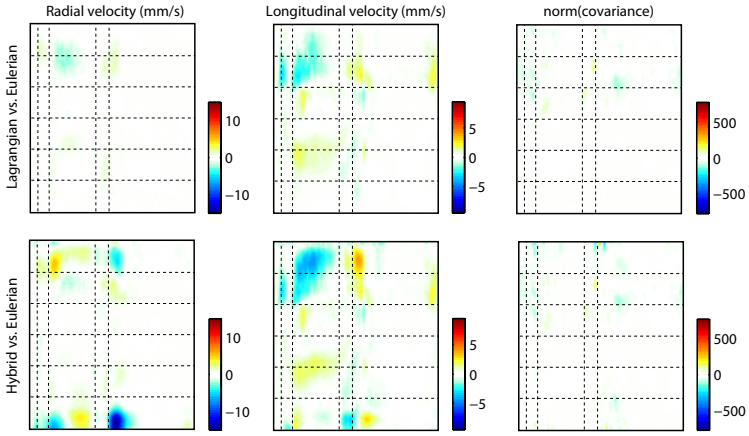


**Fig. 3:** Comparison of the *Lagrangian* and *hybrid-Eulerian* frameworks to the *Eulerian* one (voxel-wise difference of the velocity and norm of the covariance maps). First choice of reorientation action (*local rotation only*).

The comparison of the *Lagrangian* and *hybrid-Eulerian* frameworks to the *Eulerian* one is illustrated in Fig. 3, which represents the voxel-wise difference of the velocity and norm of the covariance maps for these frameworks.

As the reorientation action consists of *local rotation only*, one would expect radial/longitudinal velocities to remain radial/longitudinal with the *Lagrangian* and *Eulerian* frameworks. Little difference is observed in the velocity maps, reflecting numerical artifacts, probably introduced by the resampling performed prior to the spatiotemporal alignment process. The variability of the velocities is almost not affected, as assessed by the norm of the covariance map.

The *hybrid-Eulerian* framework is an approximation of the *Eulerian* one, which neglects the temporal (intra-subject) reorientation but not the inter-subject one. The observed changes should reflect the bias on the rotation component introduced by this approximation. Major changes are visible for the systolic and early-diastole periods, while few influence on the variability of the velocities is observed (bottom row of Fig. 3). This temporal interval corresponds to the part of the cycle of the major changes in the local orientation of the heart shape, indicating that this representation probably reflects correctly the bias on the rotation component.

**Local rotation and isotropic scaling.** The highest changes between the different choices of reorientation action (*local rotation only* and *local rotation and isotropic scaling*) are expected near end-systole and early-diastole, where the heart volume is the smallest along the cycle, and the difference to the beginning of the cycle is the highest. These changes reflect that the two reorientation actions differ by a scaling factor. This is actually observed in Fig. 4, major differences being visible for the longitudinal velocities, of higher magnitude in comparison

This a pre-print version.
The final document is available at http://www.springerlink.com



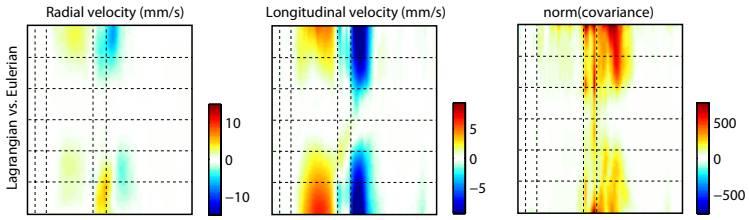


**Fig. 4:** Comparison of the *local rotation and isotropic scaling* and *local rotation only* reorientation actions for the *Eulerian* framework (voxel-wise difference of the velocity and norm of the covariance maps).

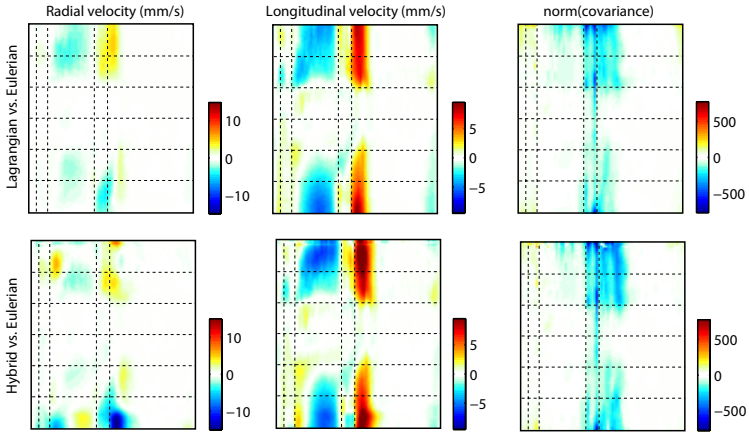


**Fig. 5:** Comparison of the *Lagrangian* and *hybrid-Eulerian* frameworks to the *Eulerian* one (voxel-wise difference of the velocity and norm of the covariance maps). Second choice of reorientation action (*local rotation and isotropic scaling*).

to the radial ones. Note that this dissymmetry is also visible on the norm of the covariance map.

The first row of Fig. 5 indicates that the *Lagrangian* and *Eulerian* frameworks mainly differ in the spatiotemporal regions of highest velocities. The sign of the difference in velocities is the opposite of the sign of the velocities, highest changes being observed near end-systole and early-diastole (as assessed by the norm of the covariance map). This is actually conform to what we could expect: these frameworks either bring the data to time $t = 0$ or $t \neq 0$, and differences in the scaling of velocities (as the reorientation action choice here is the *local rotation and isotropic scaling*) will be the highest where the heart volume is the smallest along the cycle, and the difference to the beginning of the cycle is the highest.

The second row of Fig. 5 reflects the bias introduced by the use of the *hybrid-Eulerian* scheme with respect to the *Eulerian* one. The difference pattern is very similar to the one observed between the *Lagrangian* and the *Eulerian* schemes,

This a pre-print version.
The final document is available at http://www.springerlink.com



but here differences reflect the error of neglecting the intra-subject transform, and not just that the comparison is made in another system of coordinates.

## 4 Discussion and conclusion

In the present paper, we discussed the changes induced by the choice of a specific reorientation framework (*Lagrangian*, *Eulerian*, or a compromise between both [*hybrid-Eulerian*]) for the comparison of cardiac image sequences. Experiments allowed understanding the differences between each of these frameworks and their consequences on the comparison of myocardial velocities.

The experiments first confirmed that both choices of *Eulerian* or *Lagrangian* reorientation frameworks are possible, non-expected differences between both coming from the numerical errors inherent to the spatiotemporal resampling of the myocardial velocities prior to the reorientation process.

Then, they also showed the limitations of an approximation of the Eulerian framework (denoted *hybrid-Eulerian* here), which would reorient the *Eulerian* velocities according to the same transform mapping subject $k$ to the reference at time $t = 0$. This introduces non-negligible artifacts, showing that the intra-subject transformation certainly needs to be taken into account for cardiac applications. Note however that this depends on the algorithm used to track the sequences along time: the propagation of numerical errors may be higher when getting closer to the end of the cycle, and in particular higher than the bias introduced by the *hybrid-Eulerian* scheme, which in this case could still be a reasonable option.

Finally, the experiments discussed the choice of a reorientation action, showing the differences introduced by the presence of a local scaling factor against a *local rotation only* action. However, the choice of a reorientation action is still an open question for cardiac studies (even in the case we had access to the whole Jacobian of the mapping to the reference to perform *push-forward*). In particular, we currently do not know if the local information (motion and deformation) should be rescaled or not, as the cardiac function does not only depend on the heart size and shape [3]: should the myocardial velocities of patients with normal cardiac motion and deformation, but dilated or hypertrophic heart, be rescaled and how? Note that in the present paper, the reorientation action is the same for the intra- and inter-subject transforms, but this choice should probably be revised to provide elements of response to this last question. A study computing the influence of the chosen reorientation action on other statistics, e.g. a distance between individuals and the healthy population [9], would certainly complement the discussion of the present paper.

**Acknowledgments** This work was supported by the Spanish Industrial and Technological Development Center (cvREMOD CEN-20091044).

This a pre-print version.
The final document is available at http://www.springerlink.com



## References

1. D. Adam, A. Landesberg, E. Konyukhov, P. Lysyansky, O. Lichtenstein, N. Smirin, and Z. Friedman. On changing coordinate systems for longitudinal tensor-based morphometry. In *Proc. IEEE Computers in Cardiology*, pages 337–40, 2004.
2. V. Behar, D. Adam, P. Lysyansky, and Z. Friedman. The combined effect of non-linear filtration and window size on the accuracy of tissue displacement estimation using detected echo signals. *Ultrasound*, 41(9):743–53, 2004.
3. B. Bijnens, M. Cikes, C. Butakoff, M. Sitges, and F. Crispi. Myocardial motion and deformation: What does it tell us and how does it relate to function? *Fetal Diagnosis and Therapy*, 2012. In press.
4. M. N. Bossa, E. Zacur, and S. Olmos. On changing coordinate systems for longitudinal tensor-based morphometry. In *Proc. Spatio-temporal Image Analysis for Longitudinal and Time-Series Image Data, MICCAI'10 Workshop*, 2010.
5. B. C. Davis, P. T. Fletcher, E. Bullitt, and S. Joshi. Population shape regression from random design data. *International Journal of Computer Vision*, 90:255–66, 2010.
6. M. De Craene and G. Piella. An implementation of TDFFD and LDFFD algorithms. *Insight Journal*, 63, 2012. `http://hdl.handle.net/10380/3345`.
7. M. De Craene, G. Piella, O. Camara, N. Duchateau, E. Silva, A. Doltra, J. Dhooge, J. Brugada, M. Sitges, and A. F. Frangi. Spatiotemporal diffeomorphic free-form deformation: Application to motion and strain estimation from 3D echocardiography. *Medical Image Analysis*, 16(2):427–50, 2012.
8. N. Duchateau, M. De Craene, G. Piella, and A. F. Frangi. Constrained manifold learning for the characterization of pathological deviations from normality. 2012. Under review.
9. N. Duchateau, M. De Craene, G. Piella, E. Silva, A. Doltra, M. Sitges, B. H. Bijnens, and A. F. Frangi. A spatiotemporal statistical atlas of motion for the quantification of abnormal myocardial tissue velocities. *Medical Image Analysis*, 15:316–28, 2011.
10. S. Durrleman, X. Pennec, A. Trouvé, G. Gerig, and N. Ayache. Spatiotemporal atlas estimation for developmental delay detection in longitudinal datasets. In *Proc. International Conference on Medical Image Computing and Computer Assisted Intervention, LNCS vol. 5761*, pages 297–304, 2009.
11. B. K. Fornwalt. The dyssynchrony in predicting response to cardiac resynchronization therapy: A call for change. *Journal of the American Society of Echocardiography*, 24:180–4, 2011.
12. J. A. Glaunes. *Transport par difféomorphismes de points, de mesures et de courants pour la comparaison de formes et l'anatomie numérique*. Phd thesis, Université Paris 13, 2005.
13. G. Hart, Y. Shi, H. Zhu, M. Sanchez, M. Styner, and M. Niethamme. DTI longitudinal atlas construction as an average of growth models. In *Proc. Spatio-temporal Image Analysis for Longitudinal and Time-Series Image Data, MICCAI'10 Workshop*, 2010.
14. C. Hoogendoorn, T. Whitmarsh, N. Duchateau, F. M. Sukno, M. De Craene, and A. F. Frangi. A groupwise mutual information metric for cost efficient selection of a suitable reference in cardiac computational atlas construction. In *Proc. SPIE International Conference on Medical Imaging*, page 76231R, 2010.
15. A. R. Khan, A. Trouvé, and M. F. Beg. Cross-sectional analysis of anatomical shape change over time via statistics on 4D within-subject flows. In *Proc. Spatio-temporal*

This a pre-print version.
The final document is available at http://www.springerlink.com



*Image Analysis for Longitudinal and Time-Series Image Data, MICCAI'10 Workshop*, 2010.
16. G. Langs, G. Kasprian, E. Dittrich, M. Bittner, P. C. Brugger, and D. Prayer. Group-wise spatio-temporal registration and segmentation of fetal cortical surface development. In *Proc. Spatio-temporal Image Analysis for Longitudinal and Time-Series Image Data, MICCAI'10 Workshop*, 2010.
17. M. Leitman, P. Lysyansky, S. Sidenko, V. Shir, E. Peleg, M. Binenbaum, E. Kaluski, R. Krakover, and Z. Vered. Two-dimensional strain-a novel software for real-time quantitative echocardiographic assessment of myocardial function. *Journal of the American Society of Echocardiography*, 17:1021–9, 2004.
18. M. Lorenzi, N. Ayache, X. Pennec, and the Alzheimer's Disease Neuroimaging Initiative. Schild's ladder for the parallel transport of deformations in time series of images. In *Proc. Information Processing in Medical Imaging, LNCS vol. 6801*, pages 463–74, 2011.
19. M. Lorenzi and X. Pennec. Geodesics, parallel transport and one-parameter subgroups for diffeomorphic image registration. In *Proc. Mathematical Foundations of Computational Anatomy, MICCAI'11 Workshop*, pages 64–74, 2011.
20. T. H. Marwick, C.-M. Yu, and J. P. Sun. *Myocardial Imaging: Tissue Doppler and Speckle Tracking*. Wiley-Blackwell, 2007.
21. M. I. Miller and A. Qiu. The emerging discipline of computational functional anatomy. *Neuroimage*, 45:S16–39, 2009.
22. V. Mor-avi, R. M. Lang, L. P. Badano, M. Belohlavek, N. M. Cardim, G. Derumeaux, M. Galderisi, T. Marwick, S. F. Nagueh, P. P. Sengupta, R. Sicari, O. A. Smiseth, B. Smulevitz, M. Takeuchi, J. D. Thomas, M. Vannan, J.-U. Voigt, and J. L. Zamorano. Current and evolving echocardiographic techniques for the quantitative evaluation of cardiac mechanics. *Journal of the American Society of Echocardiography*, 24:277–313, 2011.
23. X. Pennec and M. Lorenzi. Which parallel transport for the statistical analysis of longitudinal deformations? In *Proc. Colloque GRETSI*, 2011.
24. D. Perperidis, R. H. Mohiaddin, and D. Rueckert. Spatio-temporal free-form registration of cardiac MR image sequences. *Medical Image Analysis*, 9:441–56, 2005.
25. J.-M. Peyrat, H. Delingette, M. Sermesant, C. Xu, and N. Ayache. Registration of 4D cardiac CT sequences under trajectory constraints with multichannel diffeomorphic demons. *IEEE Transactions on Medical Imaging*, 29:1351–68, 2010.
26. A. Qiu, M. Albert, L. Younes, and M. I. Miller. Time sequence diffeomorphic metric mapping and parallel transport track time-dependent shape changes. *Neuroimage*, 45:S51–60, 2009.
27. A. Qiu, L. Younes, M. I. Miller, and J. G. Csernansky. Parallel transport in diffeomorphisms distinguishes the time-dependent pattern of hippocampal surface deformation due to healthy aging and the dementia of the Alzheimer's type. *NeuroImage*, 40:68–76, 2008.
28. A. W. Toga, P. M. Thompson, S. Mori, K. Amunts, and K. Zilles. Towards multimodal atlases of the human brain. *Nature Reviews Neuroscience*, 7:952–66, 2006.
29. A. Trouvé and F. X. Vialard. Shape splines and stochastic shape evolutions: A second order point of view. *Quarterly of Applied Mathematics*, 70:219–51, 2012.
30. L. W. Tu. *An Introduction to Manifolds*, chapter 14. Springer, 2007.
31. F. X. Vialard and A. Trouvé. A second-order model for time-dependent data interpolation: Splines on shape spaces. In *Proc. Spatio-temporal Image Analysis for Longitudinal and Time-Series Image Data, MICCAI'10 Workshop*, 2010.
32. A. A. Young and A. F. Frangi. Computational cardiac atlases: from patient to population and back. *Experimental Physiology*, 94:578–96, 2009.